

# Investigation of Wear Anisotropy in a Severely Deformed Al-Al<sub>3</sub>Ti Composite

SHIMAA EL-HADAD, HISASHI SATO, and YOSHIMI WATANABE

In the current investigation, Al-Al<sub>3</sub>Ti composite was processed by equal channel angular pressing (ECAP). ECAP was carried out using routes A and B<sub>C</sub> up to eight passes of deformation. It was observed that increasing the number of ECAP passes causes fragmentation of Al<sub>3</sub>Ti platelet particles and decreases their sizes compared to their original sizes in the undeformed Al-Al<sub>3</sub>Ti specimens. Moreover, the microstructure of route A-ECAPed Al-Al<sub>3</sub>Ti composite samples showed a strong alignment of the fragmented Al<sub>3</sub>Ti particles parallel to the pressing axis. On the other hand, ECAPed Al-Al<sub>3</sub>Ti alloy specimens by route B<sub>C</sub> have a relatively homogeneous distribution of Al<sub>3</sub>Ti particles. Because of the platelet Al<sub>3</sub>Ti particle fragmentation by ECAP, all the ECAPed specimens showed small anisotropy in their wear property in spite of this observed anisotropic microstructure induced by route A-ECAP.

DOI: 10.1007/s11661-012-1127-3

© The Minerals, Metals & Materials Society and ASM International 2012

## I. INTRODUCTION

ALUMINUM based composites containing aluminate particles were reported to possess higher wear resistance and lower friction with increasing volume fraction of the reinforcement particles. Compared to ceramic reinforcements, employing aluminate in Al matrix composites as wear resistant reinforcement has advantages.<sup>[1]</sup> In addition to the aluminate's high hardness, elastic modulus, melting temperature, and thermal stability, the thermal expansion coefficients of some of these intermetallics are much closer to those of Al alloys. This smaller difference in thermal expansion coefficients lowers the residual stresses at the reinforcements/matrix interfaces when the composite is exposed to thermal cycle and, hence, guarantees a lower degree of failure.<sup>[2]</sup>

Of these composites, Al-Al<sub>3</sub>Ti composites containing Al<sub>3</sub>Ti intermetallics are potential candidates as tribological materials.<sup>[3]</sup> Since the Al<sub>3</sub>Ti particles in this composite are platelet in shape, it is expected that any deformation process aligning these particles in a certain direction would result in an anisotropic wear property.

Severe plastic deformation (SPD) of metals and alloys was reported to refine their structures by the intensive plastic strain imposed on the samples.<sup>[4]</sup> Moreover, some research revealed the influence of SPD intensive strain on the microstructure orientation in some metallic alloys.<sup>[5]</sup> This oriented microstructure may result in anisotropic mechanical properties in the deformed samples, as previously observed.<sup>[6]</sup> Therefore, if a

severely deformed Al-Al<sub>3</sub>Ti composite was selected for tribological applications, the anisotropy of its wear property should be carefully investigated.

Equal-channel angular pressing (ECAP) (at present) is one of the developed SPD methods.<sup>[7]</sup> The ECAP process has the advantage that different slip systems can be introduced by rotating the samples.<sup>[8]</sup> In the case of route A, the sample is pressed repetitively without rotation, which results in accumulated unidirectional shear strain in the sample.<sup>[9]</sup> In contrast, route B<sub>C</sub> is done by rotating the specimen 90 deg in the same sense, and a homogeneous strain can be imposed through four passes.<sup>[10]</sup> Therefore, route A forms an anisotropic structure, while route B<sub>C</sub> develops a homogeneous structure.<sup>[11]</sup>

Zhang *et al.*<sup>[12]</sup> studied an ECAPed Al-5.7 wt pct Ni eutectic alloy processed through route B<sub>C</sub> and route A methods. It was found that after ECAP processing by route B<sub>C</sub>, fine Al<sub>3</sub>Ni particles were homogeneously dispersed in the Al matrix and the samples showed no clear anisotropy in their tensile properties. After ECAP processing by route A, however, the eutectic textures containing  $\alpha$ -Al and Al<sub>3</sub>Ni fibrous dispersoids have highly anisotropic distribution and are proven to have significant anisotropy in tensile properties.

The microstructure and texture evolution of an Al-Al<sub>3</sub>Ti composite ECAPed with routes A and B<sub>C</sub> were investigated by Watanabe *et al.*<sup>[13]</sup> According to their study, the microstructure of ECAPed samples by route A has highly anisotropic distribution of Al<sub>3</sub>Ti particles, while route B<sub>C</sub> samples have homogeneous distribution of Al<sub>3</sub>Ti particles.

Considering the wear property of the ECAPed Al-Al<sub>3</sub>Ti composite based on the distribution of Al<sub>3</sub>Ti particles, it is expected that route A-ECAPed Al-Al<sub>3</sub>Ti composite will have anisotropy in its wear property. This is because the mechanical properties of the particle-reinforced composite depend on the distribution and orientation of the particles, as described earlier.<sup>[14,15]</sup>

SHIMAA EL-HADAD, Researcher, is with the Central Metallurgical Research & Development Institute, Helwan-El, Tebbin, Cairo 11.421, Egypt. Contact e-mail: shimaam@yahoo.com HISASHI SATO, Associate Professor, and YOSHIMI WATANABE, Professor, are with the Department of Engineering Physics, Electronics and Mechanics, Graduate School of Engineering, Nagoya Institute of Technology, Nagoya 466-8555, Japan.

Manuscript submitted September 15, 2011.

Article published online May 15, 2012

In this study, Al-11 vol pct  $\text{Al}_3\text{Ti}$  composite was processed by ECAP with routes A and  $B_C$  up to eight passes. Using the ECAPed Al- $\text{Al}_3\text{Ti}$  composites deformed with different routes, the anisotropy in the wear property of ECAPed Al- $\text{Al}_3\text{Ti}$  composites was investigated. In spite of the alignment of  $\text{Al}_3\text{Ti}$  platelet particles to the shearing direction during ECAP, a small anisotropy in the wear property of the deformed Al- $\text{Al}_3\text{Ti}$  composites was observed.

## II. EXPERIMENTAL PROCEDURE

### A. Preparation of ECAPed Al- $\text{Al}_3\text{Ti}$ Samples

#### 1. Casting

Prior to processing by ECAP, rod-shaped ECAP specimens of Al-5 mass pct Ti alloy with a diameter of 10 mm and a length of 60 mm were prepared by casting at 1023 K (750 °C) in a metallic mold. The as-cast specimens were then machined to obtain a smooth surface. In order to stand with the severe deformation during ECAP, the specimens were homogenized at 823 K (550 °C) for 1 hour and subsequently air cooled.

### B. Deformation

An ECAP die fabricated from tool steel with two circular cross-sectional channels intersecting at 90 deg angle and a 36 deg outer arc of curvature was used, as shown in Figure 1. The ECAP was conducted with a pressing speed of 4 mm/min at room temperature using  $\text{MoS}_2$  as lubricant. An equivalent strain of about 1.0 was introduced into the sample for each pass through die.<sup>[16]</sup> Using the rod-shaped Al- $\text{Al}_3\text{Ti}$  composites, ECAP was carried out up to eight passes by route A and route  $B_C$ .

#### 1. Microstructure investigation of specimens after ECAP

The ECAPed samples were cut along the pressing axis from its central position to obtain sections for microstructure and hardness investigations. Scanning electron microscopy (SEM) was used to observe the distribution of  $\text{Al}_3\text{Ti}$  particles in the ECAPed samples at random positions. The average length of  $\text{Al}_3\text{Ti}$  particles was calculated using the linear intercept method. The intercept lines were plotted horizontally and vertically on magnified SEM images taken randomly for the ECAPed samples. The particle's aspect ratio was determined using image analysis software. The aspect ratio is defined as the ratio of maximum and minimum lengths of the rectangle with smallest area that can be drawn around the particle. The angle between the fragmented  $\text{Al}_3\text{Ti}$  particle group and the deformation direction was measured at random positions in order to study the effect of ECAP on the particle alignment.

#### 2. Wear tests of ECAPed Al- $\text{Al}_3\text{Ti}$ samples

To study the anisotropy of the wear property of the ECAPed samples, two kinds of specimens were cut at different directions relative to the deformation axis. The short specimen has a wear plane parallel to the

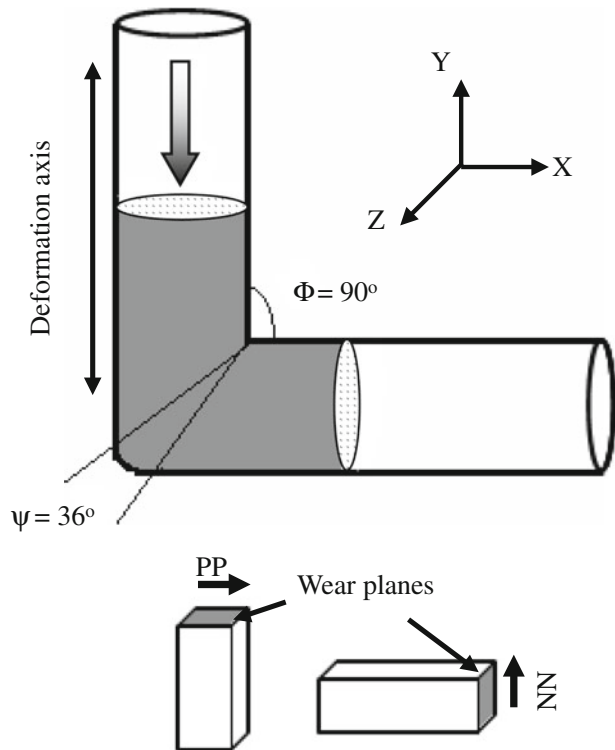


Fig. 1—Schematic illustration of ECAP showing the wear test samples and the wear directions: PP and NN.

deformation axis, while the long one was cut normal to this axis. The short and long samples have dimensions of 3.5 mm × 3.5 mm × 8 mm and 3.5 mm × 3.5 mm × 20 mm, respectively. The wear tests were carried out in X and Y directions, named PP and NN, respectively, as also shown in Figure 1. The wear tests were performed using block-on-disc type wear test. Dry wear test conditions were applied using S45C counter disc with 170 Hv hardness. The test was made under reciprocal line movement. The amplitude distance of the reciprocal movement was 26 mm and its frequency was 150 cycle/min. The load and total distance for the wear tests was 1.0 kgf and 0.468 km, respectively. The amount of wear was evaluated by weighing the samples before and after wear test.

## III. RESULTS AND DISCUSSION

### A. Microstructure Aspects of ECAPed Al- $\text{Al}_3\text{Ti}$ Composite

Figure 2(a) is an SEM micrograph showing the original microstructure of Al- $\text{Al}_3\text{Ti}$  composite, where coarse  $\text{Al}_3\text{Ti}$  platelet particles<sup>[17]</sup> were observed randomly distributed in the Al matrix. Figures 2(b) and (c) show the microstructure of Al- $\text{Al}_3\text{Ti}$  composite ECAPed by routes A and  $B_C$ , respectively, at four and eight passes of deformation observed on the plane parallel to the pressing axis. The angle  $\theta$  in these figures is the angle

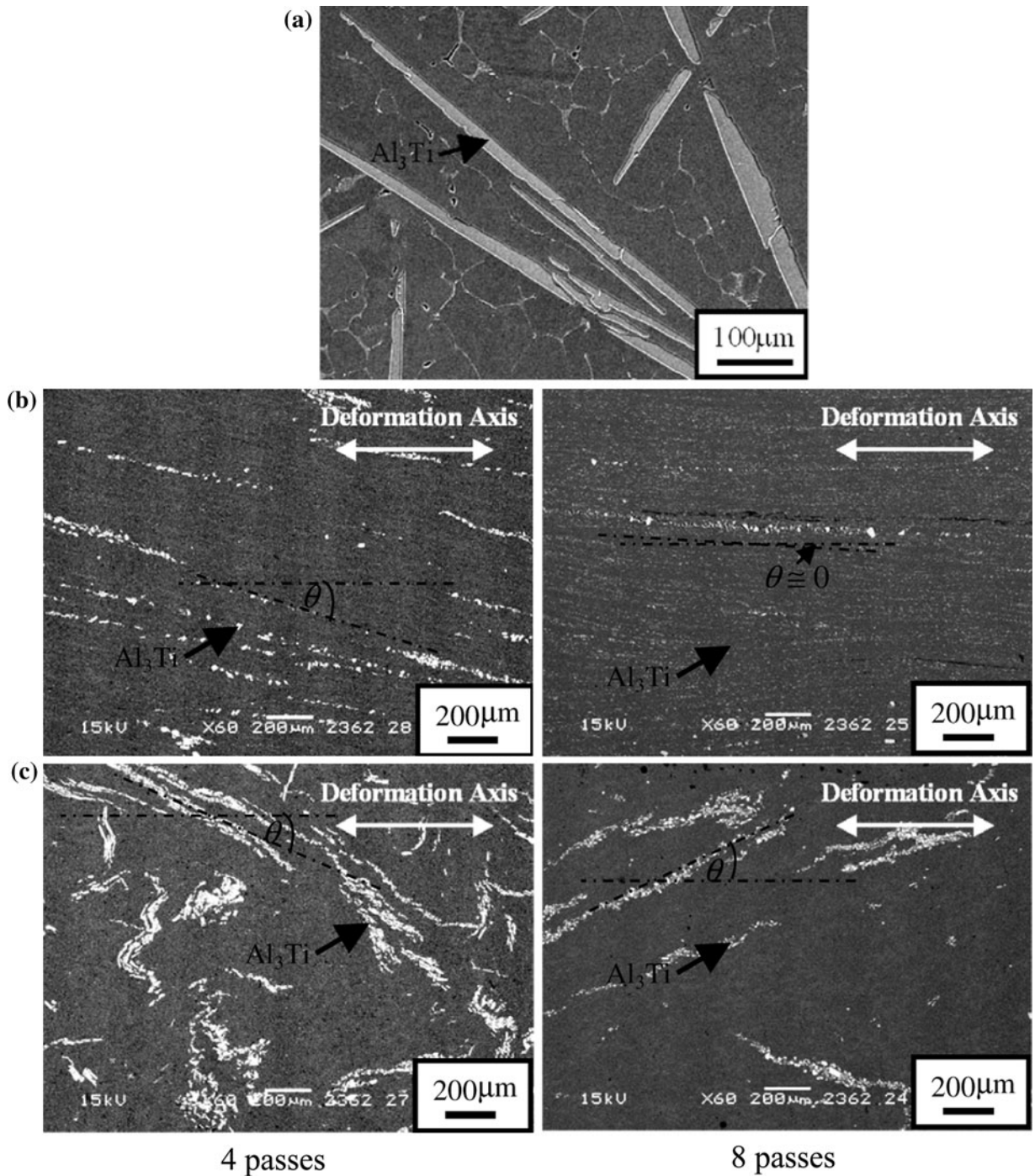


Fig. 2—SEM photographs showing microstructures of (a) as-cast Al-Al<sub>3</sub>Ti composite, (b) route A, and (c) route B<sub>C</sub> ECAPed samples.

between the deformation axis and the axis of an Al<sub>3</sub>Ti particle group. After the as-cast Al-Al<sub>3</sub>Ti composite samples were deformed under the large strains of ECAP, the Al<sub>3</sub>Ti platelet particles were severely fragmented and granular Al<sub>3</sub>Ti particles were observed. Consequently, the particles' sizes and their aspect ratios are expected to show a remarkable decrease when the deformation proceeds to higher strains.

Figures 3(a) and (b) show the average sizes of Al<sub>3</sub>Ti particles and their aspect ratios as a function of the number of ECAP passes. It is remarked that the size of Al<sub>3</sub>Ti particles in both of the specimens deformed with routes A and B<sub>C</sub> decreased with increasing the number of ECAP passes, as shown in Figure 3(a). In addition, the aspect ratio of Al<sub>3</sub>Ti particles steeply decreased when they were deformed using both ECAP routes

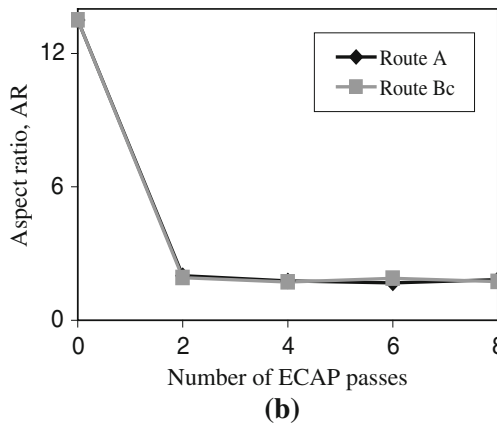
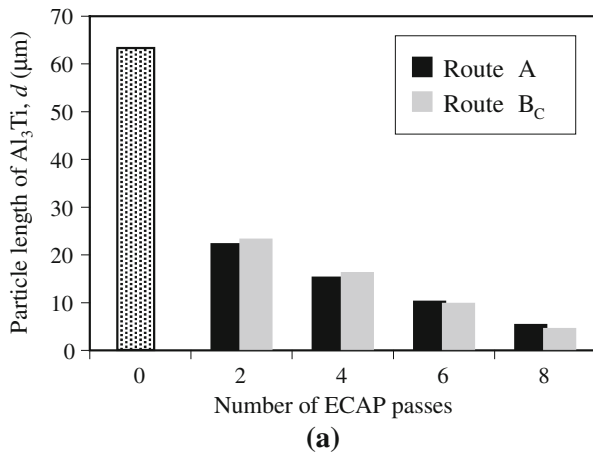


Fig. 3—Quantitative measurements of (a) mean size and (b) aspect ratio of Al<sub>3</sub>Ti particles vs number of ECAP passes on the plane parallel to the pressing axis.

(Figure 3(b)). Moreover, the common shape of the Al<sub>3</sub>Ti particle is changed from platelet to granular shape, as can be observed from the magnified micrograph of the route A sample after four passes of deformation, as shown in Figure 4.

Comparing the microstructure of route A and B<sub>C</sub> samples at eight passes of deformation, micrographs of route A (Figure 2 (b)) showed fine granular Al<sub>3</sub>Ti particles strongly aligned along the deformation axis, and the initial shape of these Al<sub>3</sub>Ti particles was not observed anymore. On the other hand, in ECAPed specimens with route B<sub>C</sub>, the alignment of the Al<sub>3</sub>Ti particles remained unchanged when the strain increased from 4 to 8. This difference of microstructure comes from the type of strain induced by ECAP. Route B<sub>C</sub> accumulates a multidirectional shear strain in the samples, while route A deforms it through a unidirectional strain.<sup>[8]</sup> Therefore, the ECAPed microstructure will be different.

Similar to short-fiber-reinforced composites, the orientation of Al<sub>3</sub>Ti platelet particles is expected to play an essential role in establishing the behavior of the composite. Although the intent of most processing procedures is to produce random fiber orientation, fabrication

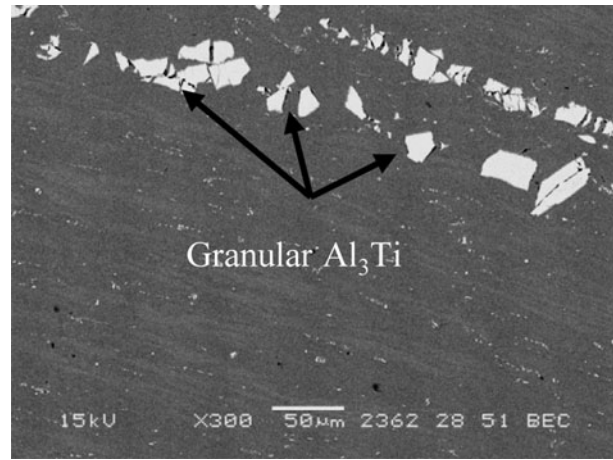


Fig. 4—Magnified SEM micrograph of the ECAPed Al-Al<sub>3</sub>Ti samples after four passes A.

kinetics can induce partial orientations, which give rise to anisotropic (*i.e.*, directionally dependent) properties.<sup>[18]</sup> This degree of anisotropy may vary depending on the fabrication conditions. In the current ECAPed Al-Al<sub>3</sub>Ti composite samples, the microstructure showed different degrees of anisotropy when different processing routes were used. The sensitivity of the properties of short-fiber-reinforced composites to processing induced fiber orientation led some researchers to quantitatively calculate the degree of fiber orientation. A Herman's orientation parameter,  $f_p$ , proposed by McGee and McCullough<sup>[18]</sup> was used in the current experiments to evaluate the microstructure anisotropy after ECAP:

$$f_p = [2 \langle \cos^2 \theta \rangle - 1], \langle \cos^2 \theta \rangle = \int_{-\pi/2}^{\pi/2} \cos^2 \theta n(\theta) d\theta \quad [1]$$

where  $\theta$  is the angle between the deformation axis and the axis of an Al<sub>3</sub>Ti particle group, as shown in Figure 2. The term  $n(\theta)$  is the orientation distribution function that specifies the fraction of particles within the angular element  $d\theta$ . The parameter  $f_p$  becomes 0 for a random distribution, and it becomes 1 for perfect alignments with the axis of Al<sub>3</sub>Ti particle groups parallel to the deformation axis.<sup>[19]</sup> Figure 5 shows the variation of  $f_p$  as a function of the number of ECAP passes evaluated on the plane parallel to the deformation axis. It is clear that the behavior of  $f_p$  for ECAPed Al-Al<sub>3</sub>Ti samples is different between routes A and B<sub>C</sub>. In both of the ECAPed specimens at two passes,  $f_p$  was around 0.4 and then this value continuously increased with further deformation by route A. The alignment of Al<sub>3</sub>Ti particles becomes almost parallel to the deformation axis at eight passes of ECAP. This is because of the reported unidirectional shear strain provided by ECAP deformation using route A.<sup>[20]</sup> When the number of passes increases, this unidirectional strain accumulates and can be translated to microstructural anisotropy, as

shown in the microstructure of route A ECAPed samples of Figure 2.

In the case of route B<sub>C</sub>,  $f_p$  at two and six passes showed relatively larger  $f_p$ , while at four and eight passes, smaller  $f_p$  was observed. However, a relatively constant trend can be considered for the overall  $f_p$  values from two to eight passes of ECAP. This result is in accordance with the reported microstructural homogeneity of route B<sub>C</sub> ECAPed samples.<sup>[21]</sup> Since ECAP using route B<sub>C</sub> induces a multidirectional shear

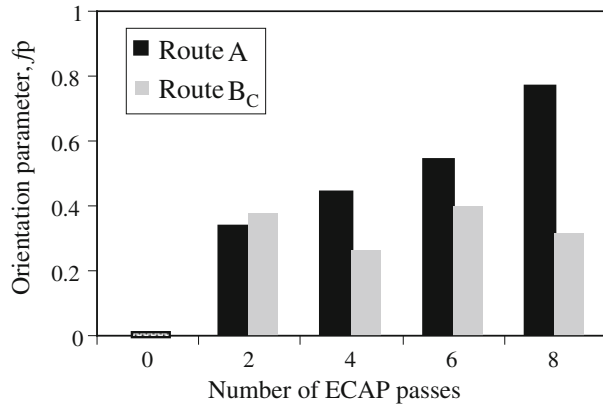


Fig. 5—Change in the calculated orientation parameter of the ECAPed Al-Al<sub>3</sub>Ti samples with increasing number of ECAP passes.

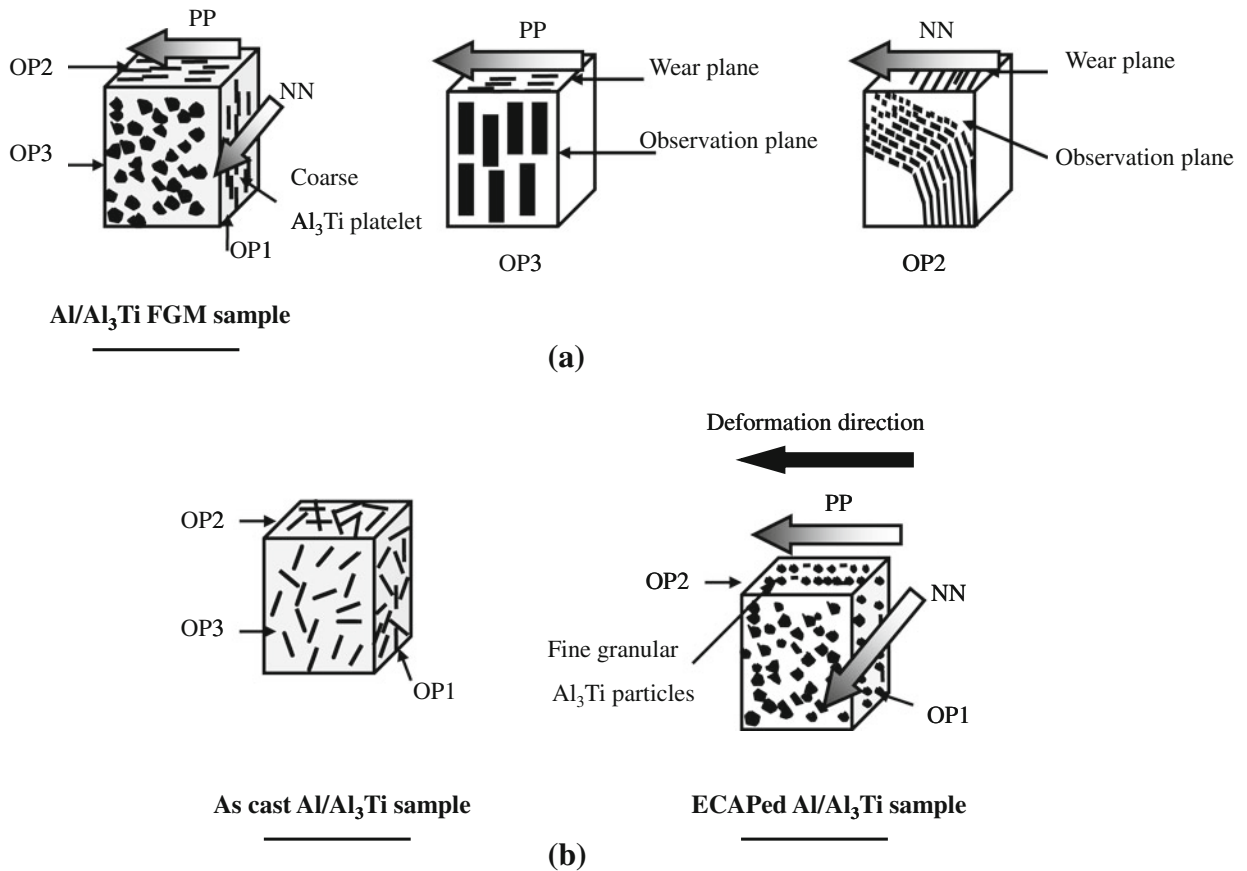


Fig. 6—Schematic illustration of (a) Al-Al<sub>3</sub>Ti FGM, (b) ECAPed Al-Al<sub>3</sub>Ti composite, and the description of wear test directions.

strain,<sup>[20]</sup> increasing the number of ECAP passes results in homogeneous distribution of the fragmented Al<sub>3</sub>Ti particles in the Al matrix.

### B. Wear Anisotropy and Particles Orientation

According to Zmitrowicz *et al.*,<sup>[22]</sup> the anisotropic friction induces anisotropic wear; *i.e.*, the intensity of the removed mass depends on the sliding direction. This anisotropy may result from the anisotropy of mechanical properties of materials with microstructures (crystals, composites, polymers, *etc.*). Based on this, the wear resistance of a composite can show some anisotropy depending on the processing induced fibers/particles orientation.

The anisotropy in the wear property was reported for Al-Al<sub>3</sub>Ti functionally graded materials (FGMs) with aligned Al<sub>3</sub>Ti particles.<sup>[23]</sup> In this study, the anisotropic wear property of the FGMs was dependent on the applied wear direction relative to Al<sub>3</sub>Ti particles. A greater anisotropy in wear resistance was found for specimens with a larger orientation parameter. This is because Al<sub>3</sub>Ti particles were groups of coarse platelet particles aligned normal to the centrifugal force direction and distributed gradually in the fabricated FGMs. The schematic illustration of the Al-Al<sub>3</sub>Ti FGM sample is shown in Figure 6(a), where the coarse aligned Al<sub>3</sub>Ti platelet particles can be observed on planes (OP1 and OP2) of the sample.

In the current ECAPed Al-Al<sub>3</sub>Ti composite, Al<sub>3</sub>Ti particle groups were aligned in a direction close to the deformation direction. However, the fragmentation of Al<sub>3</sub>Ti platelet particles by the large strain of ECAP refined their size and changed their shape to the granular morphology, as obvious on planes (OP1 and OP2) shown in Figure 6(b). Comparing the reported microstructure of Al-Al<sub>3</sub>Ti FGMs<sup>[23]</sup> with the current ECAPed Al-Al<sub>3</sub>Ti composite, small anisotropy can be expected in the wear property of ECAPed Al-Al<sub>3</sub>Ti samples when tested on the PP and NN directions.

The variations in weight loss by wear of routes A and B<sub>C</sub> ECAPed samples using the block-on-disc wear test are shown in Figure 7. In the nondeformed samples, the very large intermetallic particles act as load-supporting elements preventing the soft Al matrix from becoming directly involved in the wear process, similar to particulate-reinforced Al matrix composites.<sup>[24]</sup> Upon further deformation, with a continued reduction in the size of Al<sub>3</sub>Ti particles and their alignment in bands along the deformation direction, a decrease in the wear resistance is observed in the PP direction up to four of ECAP. This is due to the loss of load bearing capabilities of the particles, which caused an increased wear rate accordingly. However, with increasing the applied strain to 6, the particles will be further refined and show their strengthening effect on the matrix, reducing the weight loss in the direction parallel to the deformation direction.<sup>[1]</sup> This was not the case for the NN direction, where the wear rate increased at two passes of deformation and then remained almost constant with increasing applied strain. This can be attributed to the observed banded microstructure shown in Figures 2(b) and (c), which in turn makes the contact between the sample block and the disc, which occurs in successive bands of reinforced and nonreinforced regions.

Comparing the weight loss for the two test directions shown in Figure 7, it is observed that the wear property in the deformation direction, PP, is consistently better than that for the NN direction for both route A and B<sub>C</sub> samples. However, these differences in the wear property between NN and PP directions are small considering the error bars for the plotted points. Therefore, it can be said that the

ECAPed samples do not have a large anisotropic wear property regardless of the processing route.

With the preceding in mind, it is concluded that there are two main factors influencing the anisotropy in the ECAPed Al-Al<sub>3</sub>Ti samples: the particle shape (coarse platelet/fine granular) and the particle alignment to a certain direction. Figures 8(a) and (b) shows the relationship between the weight loss and the orientation parameter in the parallel and normal wear test directions, respectively. It is observed that increasing  $fp$  up to (-0.4) resulted in increased weight loss in both the PP and NN directions. However, the weight loss value decreased with further increase of the orientation parameter. This is because of the associated decrease in the particle size and aspect ratio with increasing the number of ECAP passes, as shown in Figure 3.

In order to understand the difference in wear anisotropy among the Al-Al<sub>3</sub>Ti FGMs and ECAPed Al-Al<sub>3</sub>Ti composite, theoretical wear models discussed in Reference 25 can be helpful. Archard<sup>[26]</sup> formulated the wear equation of the form

$$W = \frac{p_n s}{H} \quad [2]$$

where the volume of the material removed ( $W$ ) is directly proportional to the sliding distance ( $s$ ), the normal pressure ( $p_n$ ), and the dimensionless wear coefficient ( $k$ ), and inversely proportional to the hardness of the surface being worn away ( $H$ ). By analogy to Archard's law, in the simplest case, wear velocities (Eq. [3]) can be defined as functions of the normal pressure ( $p_n$ ) and the sliding velocity ( $V_{AB}$ ); *i.e.*,

$$v^+ = -i_A |p_n^A| |V_{AB}| \quad \text{and} \quad v^- = -i_B |p_n^B| |V_{BA}| \quad [3]$$

where

$$|p_n^A| = |p_n^B|, V_{AB} = -V_{BA} \quad [4]$$

The coefficients  $i_A$  and  $i_B$  used in Eq. [3] are defined as dimensional wear constants or the specific wear rates.<sup>[27]</sup> If  $i_A$  and  $i_B$  are multiplied by the hardness of bodies,

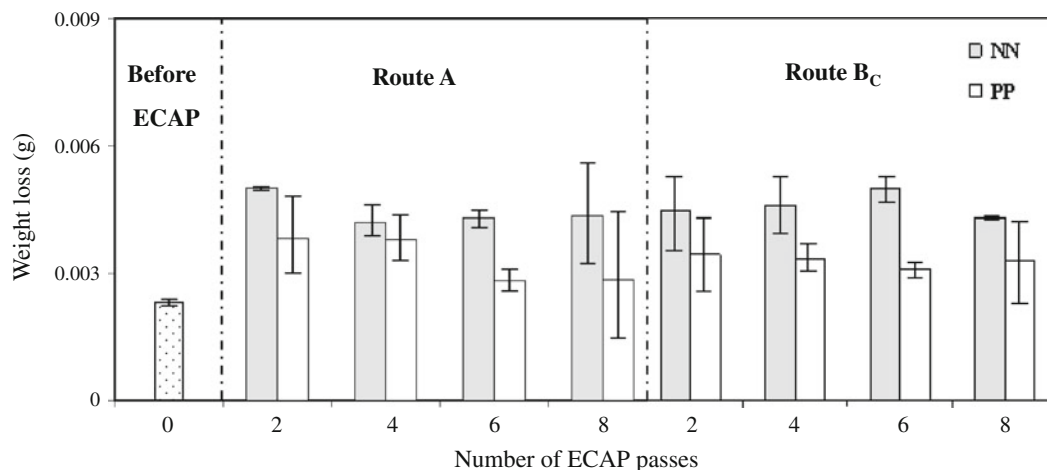


Fig. 7—Weight loss during block-on-disc wear test of routes A and B<sub>C</sub> ECAPed Al-Al<sub>3</sub>Ti alloy samples.

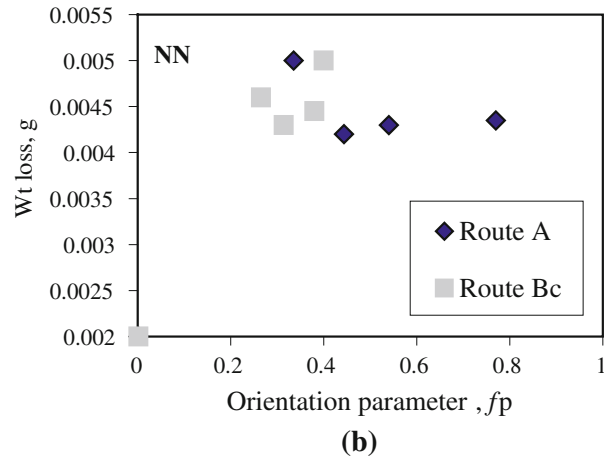
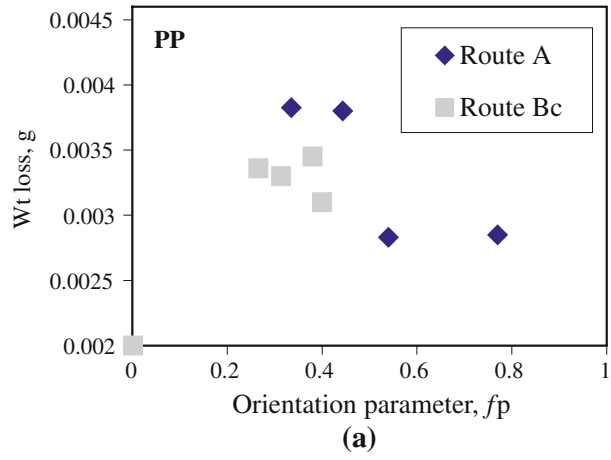


Fig. 8—Weight loss of ECAPed Al-Al<sub>3</sub>Ti samples in (a) PP and (b) NN directions vs the particle's orientation parameter.

then we get dimensionless intensities of wear  $i_A H_A$  and  $i_B H_B$ . Therefore, the hardness can be easily included in the quantitative estimation of the dimensional wear intensity coefficients  $i_A$  and  $i_B$ .

Zmitrowicz *et al.*<sup>[22,27]</sup> assumed that the wear intensity  $i_A$  is a function of the sliding direction. Following his assumption, the orientation parameter,  $fp$ , defined in Eq. [1] as the degree of the platelet particle orientation should relate to the wear intensity  $i_A$ . Using the extension of Archard law described in Reference 25,  $i_A$  and  $fp$  can be related as follows:

$$i_A = i_A(fp), fp \in (0, 1) \quad [5]$$

By substituting in Archard law (Eq. [2]), the anisotropy of wear can be explained by

$$W = \frac{p_n s}{H(fp)} \quad [6]$$

And the velocity Eq. [3] will be accordingly changed to

$$v^+ = -i_A(f_p) |p_n^A| |V_{AB}| \text{ and } v^- = -i_B(f_p) |p_n^B| |V_{BA}| \quad [7]$$

Equations [6] and [7] can be roughly applied to the case of FGM, where the platelet particles are present

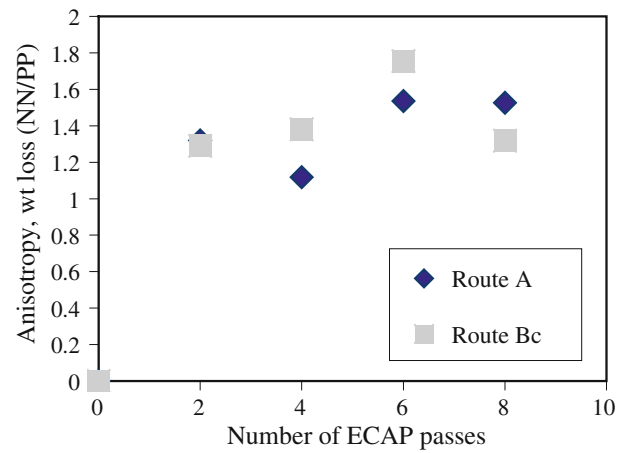


Fig. 9—Variation of wear anisotropy of ECAPed Al-Al<sub>3</sub>Ti samples with number of ECAP passes.

and the influence of  $fp$  on the wear anisotropy is quite important. In the current ECAPed samples, however, this equation is not applicable since the particle shape was altered to fine nonplatelet particles. Thus, even if the orientation parameter apparently increased, no significant change will really occur. Therefore, it is recommended in the case of ECAPed Al-Al<sub>3</sub>Ti to calculate the average hardness in the two test directions and then substitute to Archard law (Eq. [2]) separately. Representing the wear anisotropy *via* mathematical models and thus calculating the volume loss ( $W$ ) in both Al-Al<sub>3</sub>Ti FGMs and ECAPed Al-Al<sub>3</sub>Ti using the precedent equations should be a topic for future work.

In order to quantitatively explain the anisotropic wear resistance, the weight loss ratio (weight loss of direction (NN)/weight loss of direction (PP)) was calculated. We have considered that the larger the value of the weight loss ratio, the larger the anisotropy of wear resistance. Figure 9 shows the anisotropy (weight loss ratio) against the number of ECAP passes. From this figure, it is evident that the anisotropy increases with increasing the deformation up to six passes and hence increasing the particle alignment to the deformation direction. Upon further deformation, the anisotropy of the Al-Al<sub>3</sub>Ti samples decreased at eight passes of ECAP using route A and route B<sub>C</sub>. The significant increase of  $fp$  value from six to eight passes using route A, which resulted in a banded structure, as shown in Figure 2(b), was expected to increase the wear anisotropy. However, the smaller size and the lower aspect ratio of the Al<sub>3</sub>Ti particles observed at eight passes A limited the effect of increasing  $fp$  on the anisotropy of the ECAPed samples. Therefore, the samples did not show larger anisotropy at eight passes of ECAP.

#### IV. CONCLUSIONS

In this study, microstructure and wear anisotropy of Al-Al<sub>3</sub>Ti composite ECAPed by routes A and B<sub>C</sub> were investigated. Fine Al<sub>3</sub>Ti particles homogeneously dispersed in Al matrix were observed in case of route

B<sub>C</sub>-ECAPed samples. In contrast, the microstructure of route A-ECAPed samples showed a highly anisotropic distribution. In spite of this observation, all the ECAPed specimens showed small anisotropy in their wear property. Concluding, ECAP, as one of SPD processes, can alter the shape of the platelet Al<sub>3</sub>Ti particles and fragment it to very small sized granular particles. As a result, limited anisotropy of the wear property in the Al-Al<sub>3</sub>Ti composite containing platelet particles can be achieved regardless of the ECAP processing route.

## ACKNOWLEDGMENTS

This work is supported by the “Grant-in-Aid for Scientific Research on Priority Areas (19025005)” and the “Tokai Region Nanotechnology Manufacturing Cluster in Knowledge Cluster Initiative” by the Ministry of Education, Culture, Sports, Science and Technology of Japan. One of the authors (SE) acknowledges the financial support in the form of a scholarship from the Egyptian government. YW gratefully acknowledges the financial support from The Light Metal Educational Foundation Inc. of Japan.

## REFERENCES

1. J.M. Wu and Z.Z. Li: *Wear*, 2000, vol. 244, pp. 147–53.
2. M. Yamaguchi and H. Inui: in *Structural Applications of Intermetallics Compounds*, J.H. Westbrook and R.L. Fleischer, eds., John Wiley, New York, NY, 1995.
3. N.Q. Wu, G.X. Wang, Z.Z. Li, J.M. Wu, and J.W. Chen: *Wear*, 1997, vols. 203–204, pp. 155–61.
4. R.Z. Valiev, Y. Estrin, Z. Horita, T.G. Langdon, M.J. Zehetbauer, and Y.T. Zhu: *JOM*, 2006, vol. 58, pp. 33–39.
5. K. Furuno, H. Akamatsu, K. Oh-ishi, M. Furukawa, Z. Horita, and T.G. Langdon: *Acta Mater.*, 2004, vol. 52, pp. 2497–2507.
6. Y. Watanabe, H. Sato, and Y. Fukui: *Solid Mech. Mater. Eng.*, 2008, vol. 2, pp. 842–53.
7. G.J. Raab, R.Z. Valiev, T.C. Lowe, and Y.T. Zhu: *Mater. Sci. Eng. A*, 2004, vol. 382, pp. 30–34.
8. R.Z. Valiev, R.K. Islamgaliev, N.F. Kuzmina, Y. Li, and T.G. Langdon: *Scripta Mater.*, 1999, vol. 40, pp. 117–21.
9. R.Z. Valiev, R.K. Islamgaliev, and I.V. Alexandrov: *Prog. Mater. Sci.*, 2000, vol. 45, pp. 103–89.
10. R.Z. Valiev and T.G. Langdon: *Rev. Adv. Mater. Sci.*, 2006, vol. 13, pp. 15–26.
11. M. Furukawa, Y. Iwahashi, Z. Horita, M. Nemoto, and T.G. Langdon: *Mater. Sci. Eng. A*, 1998, vol. 257, pp. 328–32.
12. Z. Zhang, Y. Watanabe, and I.-S. Kim: *Mater. Sci. Technol.*, 2005, vol. 21, pp. 708–14.
13. Y. Watanabe, P.D. Sequeira, O. Sitdikov, H. Sato, Z. Zhang, and I.-S. Kim: *Mater. Sci. Forum*, 2007, vols. 561–565, pp. 251–54.
14. H. Sato and Y. Watanabe: *Mater. Sci. Forum*, 2007, vols. 561–565, pp. 659–62.
15. Y. Watanabe, R. Sato, K. Matsuda, and Y. Fukui: *Sci. Eng. Comp. Mater.*, 2004, vol. 11, pp. 185–99.
16. K. Nakashima, Z. Horita, M. Nemoto, and T.G. Langdon: *Acta Mater.*, 1998, vol. 46, pp. 1589–99.
17. Y. Watanabe, H. Eryu, and K. Matsuura: *Acta Mater.*, 2001, vol. 49, pp. 775–83.
18. S.H. McGee and R.L. McCullough: *J. Appl. Phys.*, 1984, vol. 55, pp. 1394–1403.
19. Y. Watanabe: *J. Comp. Mater.*, 2002, vol. 36, pp. 915–23.
20. T.G. Langdon: *Rev. Adv. Mater. Sci.*, 2006, vol. 13, pp. 6–14.
21. M. Furukawa, Z. Horita, and T.G. Langdon: *THERMEC*, T. Chandra, N. Wanderka, W. Reimers, and M. Lonescu, eds., Trans Tech Publications, Aedermannsdorf, Switzerland, 2009, pp. 1946–1951.
22. A. Zmitrowicz: *Z. Angew. Math. Mech.*, 1992, vol. 72, pp. 290–92.
23. Y. Watanabe, N. Yamanaka, and Y. Fukui: *Metall. Mater. Trans. A*, 1999, vol. 30A, pp. 3253–61.
24. A.T. Alpas and J. Zhang: *Metall. Trans. A*, 1994, vol. 25A, pp. 969–81.
25. A. Zmitrowicz: *J. Theor. Appl. Mech.*, 2006, vol. 44, pp. 219–53.
26. J.F. Archard: *J. Appl. Phys.*, vol. 24, pp. 981–88.
27. A. Zmitrowicz: *J. Eng. Sci.*, 1993, vol. 31, pp. 509–28.